POLARIMETRIC TWO-SCALE MODEL FOR THE EVALUATION OF BISTATIC SCATTERING FROM ANISOTROPIC SEA SURFACES

Gerardo Di Martino, Alessio Di Simone, Antonio Iodice, Daniele Riccio

Department of Electrical Engineering and Information Technology,
University of Naples "Federico II", Naples, Italy.

IGARSS 2020 - 2020 IEEE International Geoscience and Remote Sensing Symposium | 978-1-7281-6374-1/20/$31.00 ©2020 IEEE | DOI: 10.1109/IGARSS39084.2020.9324450

ABSTRACT

The Two-Scale Model (TSM) is a useful approach for the evaluation of scattering from rough surfaces. In order to model depolarization effects, TSM, in its original formulation, requires an average operation that calls for numerical integration, so strongly reducing the computation efficiency. However, in the last decade a method to analytically compute this average in closed form, named Polarimetric TSM (PTSM), was devised. More recently, the PTSM, originally applied to backscattering from statistically isotropic rough scattering surfaces, was extended to the case of anisotropic rough surfaces (A-PTSM), in order to compute backscattering from sea surfaces. Both PTSM and A-PTSM, as presented in previous work, only consider the monostatic configuration. Here, we extend A-PTSM to the more general case of bistatic scattering. In particular, we present the procedure to obtain all the elements of the bistatic polarimetric covariance matrix in closed form; we then present some numerical results with reference to the bistatic Normalized Radar Cross Sections (NRCS) in circular polarization basis, which are of interest for some recently proposed bistatic passive radar systems with GNSS signals of opportunity.

Index Terms— electromagnetic scattering from rough surfaces; sea surface scattering

1. INTRODUCTION

The Two-Scale Model (TSM) is a method, firstly proposed about fifty years ago [1-2], to compute scattering from rough surfaces [1], and in particular from sea surfaces [2]. According to this model, the scattering rough surface is represented as the superposition of a small-scale roughness, with horizontal scale of the order of wavelength and vertical deviations much smaller than wavelength, and a large-scale roughness, with horizontal scale very large with respect to wavelength and vertical deviations of the order of wavelength or higher. The Small Perturbation Method (SPM) [3] is used to compute scattering from small-scale roughness, which turns out to mainly depend on small-scale roughness spectrum, whereas Geometrical Optics (GO) [3] is employed to evaluate scattering from large-scale roughness, which turns out to mainly depend on large-scale roughness root mean square (rms) slopes. The small-scale scattering contribution is dominant in far-from-specular directions, whereas the large-scale one is dominant in near-specular directions.

If only co-polarized normalized radar cross section (NRCS) is of interest, a combination of the analytical closed form expressions of GO and SPM can be used, so that a high computation efficiency is obtained. However, if a fully polarimetric analysis of the scattered field is needed, so that cross-polarization and de-polarization effects must be modelled, then the SPM expression of scattering from small-scale roughness must be averaged over the surface slopes of the large-scale roughness. This average operation calls for numerical integration, so that computation efficiency is strongly reduced. A few years ago, however, its approximated closed-form expression was devised [4]: the so obtained fully polarimetric version of TSM was named Polarimetric TSM (PTSM), and it was applied to model soil surface scattering in the framework of soil moisture retrieval from polarimetric Synthetic Aperture Radar (SAR) data [4-6]. More recently, the PTSM, originally applied to backscattering from statistically isotropic rough scattering surfaces, was extended to the case of anisotropic rough surfaces (A-PTSM), in order to compute backscattering from sea surfaces [7-8]. Both PTSM and A-PTSM, as presented in previous works [4-8], only consider the monostatic configuration (although in [8] extension to bistatic scattering from isotropic rough surfaces has been briefly sketched). In this work we extend A-PTSM to the more general case of bistatic scattering from anisotropic rough surfaces. Specifically, after recalling the employed sea surface model (Section 2), we present the procedure to obtain all the elements of the bistatic polarimetric covariance matrix in closed form (Section 3); we then show some numerical results relative to NRCS in circular polarization basis (Section 4), and, finally, we provide some concluding remarks (Section 5).

2. SEA SURFACE MODEL

In order to implement the TSM, the power spectral density (PSD) of the small-scale roughness and the probability density function (pdf) of the large-scale roughness slopes must be specified.

The small-scale roughness two-dimensional (2D) PSD (often briefly referred to as surface spectrum) can be expressed in general as:

$$W_{2D}(\kappa,\varphi) = W(\kappa)\Phi(\kappa,\varphi) \tag{1}$$

where κ is the amplitude of the surface wavenumber vector and φ is the angle between the surface wavenumber vector and the x axis (see Fig. 1); and $W(\kappa)$ and $\Phi(\kappa,\varphi)$ are the omnidirectional part of the spectrum and the angular spreading function, respectively. Different expressions of the sea surface spectrum have been proposed in literature; here, by following the approach of [7], for the small-scale roughness we use the high-frequency part of the Elfouhaily spectrum [9]. Its full detailed expressions can be found in [7, eqs.(2-8)]; we here recall that, similarly to other sea spectra available in literature [3], in the range of surface wavenumbers of interest for microwave scattering they can be well approximated by

$$W(\kappa) \cong \frac{S_0}{\kappa^{3.5}} \quad , \tag{2}$$

$$\Phi(\kappa,\varphi) \cong \Phi(\varphi) = 1 + \Delta\cos\left[2\left(\varphi_w - \varphi\right)\right] \quad , \tag{3}$$

where S_0 and Δ are wind-speed-dependent constants [7] and φ_w is the angle between the wind direction and the x axis.

With regard to the large-scale roughness, sea surface slopes along up-wind and cross-wind directions, s_{up} and s_{cross}, are, with good approximation, zero-mean independent Gaussian random variables with variances σ_{up}^2 and σ_{cross}^2, respectively [10]. These slope variances depend both on wind speed and on the incident electromagnetic wavenumber k, that defines the cut-off scale between small- and large-scale roughness. They can be computed, by using the approach of [7], as:

$$\sigma_{up,cross}^2 \cong \sigma_{up0,cross0}^2 + \frac{S_0}{2\pi}\left(1 \pm \frac{\Delta}{2}\right)\left(\sqrt{\kappa_{cut}} - \sqrt{\kappa_{cut0}}\right) \quad , \tag{4}$$

where $\sigma_{up0,cross0}^2$ are the values obtained by using the semiempirical evaluation of [11], that holds at the frequency of 1.5 GHz, κ_{cut} is the cut-off wavenumber at the considered incident electromagnetic wave frequency, and κ_{cut0} is the cut-off wavenumber at 1.5 GHz. Here we will use $\kappa_{cut} = k/2$, but the slope variance values in (4) only slightly depend on this choice, since the bulk of the evaluation is based on the semiempirical values $\sigma_{up0,cross0}^2$.

Based on the above hypothesis on s_{up} and s_{cross}, it is easy to show [7] that surface slopes along x and y directions, s_x and s_y, are zero-mean jointly Gaussian random variables with variances

$$\begin{aligned} \sigma_x^2 &= \frac{1}{2}\left[\sigma_{up}^2 + \sigma_{cross}^2 + \left(\sigma_{up}^2 - \sigma_{cross}^2\right)\cos 2\varphi_w\right] \\ \sigma_y^2 &= \frac{1}{2}\left[\sigma_{up}^2 + \sigma_{cross}^2 - \left(\sigma_{up}^2 - \sigma_{cross}^2\right)\cos 2\varphi_w\right] \end{aligned} \tag{5}$$

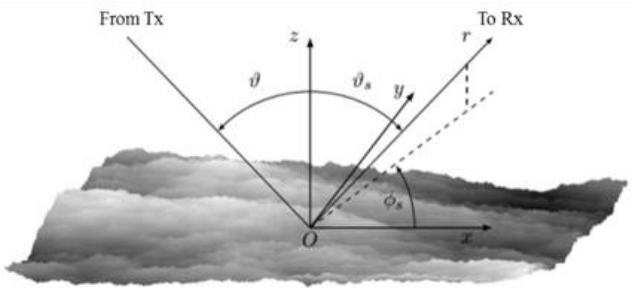

Figure 1: Geometry of the problem and coordinate system

and correlation coefficient

$$\rho = \frac{1}{2}\sin 2\varphi_w \frac{\sigma_{cross}^2 - \sigma_{up}^2}{\sigma_x \sigma_y} \quad . \tag{6}$$

3. ANISOTROPIC BISTATIC PTSM

In our version of the TSM, the overall scattering surface is modeled as a collection of randomly rough facets, whose roughness is the small-scale roughness, randomly tilted according to the slope of the large-scale roughness. The contribution from the large-scale roughness is computed via the GO, and corresponding closed-form expressions for the elements of the covariance matrix are available in literature [3]. With regard to the contribution from the small-scale roughness, the covariance scattering matrix of a tilted rough facet is computed by using the SPM, and the covariance scattering matrix of the overall surface is obtained by averaging the one of the tilted facet with respect to facet random slopes.

The SPM expression of the bistatic covariance matrix elements of the tilted facet can be expressed in the facet local reference system, i.e., in terms of the local incidence ϑ_{li} and scattering ϑ_{ls}, φ_{ls} angles, and rotation angles β_i and β_s of incidence and scattering planes, as:

$$R_{pq,rs}^{SPM} = \frac{4}{\pi}k^4 \cos^2\vartheta_{li}\cos^2\vartheta_{ls}\,\chi_{pq}\chi_{rs}^{*}\,W_{2D}\left(\bar{\kappa}_l,\bar{\varphi}_l\right) \tag{7}$$

where the subscripts p, q, r, s may each stand for h (horizontal polarization) or v (vertical polarization), so that $R_{pq,pq}$ is the NRCS σ_{pq}^0 at pq polarization. In addition, $\bar{\kappa}_l = \sqrt{\kappa_{lx}^2 + \kappa_{ly}^2}$ and $\bar{\varphi}_l = \arctan\left(\kappa_{ly}/\kappa_{lx}\right)$, with

$$\begin{aligned} \kappa_{ly} &= -k\sin\vartheta_{ls}\sin\varphi_{ls} \\ \kappa_{lx} &= -k\sin\vartheta_{ls}\cos\varphi_{ls} + k\sin\vartheta_{li} \end{aligned} \quad . \tag{8}$$

Finally,

$$\underline{\underline{\chi}}\left(\vartheta_{li},\vartheta_{ls},\varphi_{ls},\beta_i,\beta_s\right) = \underline{\underline{R_2}}\left(\beta_s\right)\cdot\begin{pmatrix} F_{hh} & F_{hv} \\ F_{vh} & F_{vv} \end{pmatrix}\cdot\underline{\underline{R_2}}^{-1}\left(\beta_i\right) \tag{9}$$

where $\underline{\underline{R_2}}\left(\beta_{i,s}\right)$ is the 2x2 rotation matrix, accounting for the rotation of the local polarization incidence and scattering

planes with respect to the global ones, and $F_{pq}(\vartheta_{li}, \vartheta_{ls}, \varphi_{ls})$ are the bistatic Bragg coefficients [3].

Then, the local incidence ϑ_{li} and scattering ϑ_{ls}, φ_{ls} angles, and rotation angles β_i and β_s of incidence and scattering planes, must be expressed in terms of global incidence ϑ_i and scattering ϑ_s, φ_s angles and of local surface slopes s_x and s_y; expressions for ϑ_{li} and β_i are already available in literature, see [7, eq.(23)], whereas the other ones are provided here:

$$\cos\vartheta_{ls} = \frac{-s_y \sin\vartheta_s \sin\varphi_s - s_x \sin\vartheta_s \cos\varphi_s + \cos\vartheta_s}{\sqrt{1+s_x^2+s_x^2}} \tag{10}$$

$$\cos\varphi_{ls} = \frac{1}{\sqrt{(\sin\vartheta_i - s_x\cos\vartheta_i)^2 + s_y{}^2}} \left(\frac{(\sin\vartheta_i - s_x\cos\vartheta_i)(\sin\vartheta_s\cos\varphi_s + s_x\cos\vartheta_s)}{\sqrt{(\sin\vartheta_s\cos\varphi_s + s_x\cos\vartheta_s)^2 + (-s_y\cos\vartheta_s - \sin\vartheta_s\sin\varphi_s)^2 + (-s_x\sin\vartheta_s\sin\varphi_s + s_y\sin\vartheta_s\cos\varphi_s)^2}} + \right.$$
$$\left. + \frac{s_y\cos\vartheta_i(-s_y\cos\vartheta_s - \sin\vartheta_s\sin\varphi_s) + s_y\sin\vartheta_i(-s_x\sin\vartheta_s\sin\varphi_s + s_y\sin\vartheta_s\cos\varphi_s)}{\sqrt{(\sin\vartheta_s\cos\varphi_s + s_x\cos\vartheta_s)^2 + (-s_y\cos\vartheta_s - \sin\vartheta_s\sin\varphi_s)^2 + (-s_x\sin\vartheta_s\sin\varphi_s + s_y\sin\vartheta_s\cos\varphi_s)^2}} \right) \tag{11}$$

$$\tan\beta_s = \frac{s_x\sin\varphi_s - s_y\cos\varphi_s}{s_y\cos\vartheta_s\sin\varphi_s + s_x\cos\vartheta_s\cos\varphi_s + \sin\vartheta_s} \quad . \tag{12}$$

Full derivation of (10-12) will be provided in [12].

At this point, bistatic covariance matrix elements of the tilted facet, (7), can be expanded in power series of facet slopes s_x and s_y; by arresting the expansion at the second order, we get:

$$R^{SPM}_{pq,rs}(\vartheta_{li}, \vartheta_{ls}, \varphi_{ls}, \beta_i, \beta_s) \cong \frac{4}{\pi} k^4 \cos^2\vartheta_i \cos^2\vartheta_s F_{pq} F^*_{rs} W_{2D}(\bar{\kappa}, \bar{\varphi}) + \\ + D^{pq,rs}_{1,0} s_x + D^{pq,rs}_{0,1} s_y + D^{pq,rs}_{2,0} s_x^2 + D^{pq,rs}_{0,2} s_y^2 + D^{pq,rs}_{1,1} s_x s_y \tag{13}$$

where

$$D^{pq,rs}_{k,n-k} = \frac{1}{n!}\binom{n}{k} \frac{\partial^n R^{SPM}_{pq,rs}}{\partial s_x{}^k \, \partial s_y{}^{n-k}}\bigg|_{s_x = s_y = 0} \quad , \tag{14}$$

$\bar{\kappa} = \sqrt{\kappa_x^2 + \kappa_y^2}$ and $\bar{\varphi} = \arctan(\kappa_y / \kappa_x)$, with

$$\kappa_y = -k \sin\vartheta_s \sin\varphi_s$$
$$\kappa_x = -k \sin\vartheta_s \cos\varphi_s + k \sin\vartheta_i, \tag{15}$$

and F_{pq} are evaluated in $\vartheta_i, \vartheta_s, \varphi_s$.

Derivatives in (14) can be analytically computed in closed form, although their expressions are rather involved and will be illustrated elsewhere [12].

Finally, bistatic covariance matrix elements of the overall surface can be obtained by averaging with respect to facet slopes:

$$< R^{SPM}_{pq,rs}(\vartheta_{li}, \vartheta_{ls}, \varphi_{ls}, \beta_i, \beta_s) > \cong \frac{4}{\pi} k^4 \cos^2\vartheta_i \cos^2\vartheta_s F_{pq} F^*_{rs} W_{2D}(\bar{\kappa}, \bar{\varphi}) + \\ + D^{pq,rs}_{2,0}\sigma_x^2 + D^{pq,rs}_{0,2}\sigma_y^2 + D^{pq,rs}_{1,1}\rho\sigma_x\sigma_y \tag{15}$$

An expression similar to (15) can be obtained in circular polarization basis. In fact, the SPM expression of the bistatic covariance matrix elements in circular polarization basis is

$$\tilde{R}^{SPM}_{PQ,RS} = \frac{4}{\pi} k^4 \cos^2\vartheta_{li} \cos^2\vartheta_{ls} \, \tilde{\chi}_{PQ} \tilde{\chi}^*_{RS} W_{2D}(\bar{\kappa}_l, \bar{\varphi}_l) \tag{16}$$

where P, Q, R and S may each stand for R (right-handed polarization) or L (left-handed polarization), and

$$\underline{\underline{\tilde{\chi}}} = \underline{\underline{U_{l\to c}}} \cdot \underline{\underline{\chi}} \cdot \underline{\underline{U_{l\to c}}}^{-1} \quad , \tag{17}$$

with $\underline{\underline{U_{l\to c}}}$ being the matrix of the linear to circular polarization basis change [13]. By proceeding as in the linear basis case, we get

$$< \tilde{R}^{SPM}_{PQ,RS}(\vartheta_{li}, \vartheta_{ls}, \varphi_{ls}, \beta_i, \beta_s) > \cong \frac{4}{\pi} k^4 \cos^2\vartheta_i \cos^2\vartheta_s \, \tilde{\chi}_{PQ} \tilde{\chi}^*_{RS} W_{2D}(\bar{\kappa}, \bar{\varphi}) + \\ + \tilde{D}^{PQ,RS}_{2,0}\sigma_x^2 + \tilde{D}^{PQ,RS}_{0,2}\sigma_y^2 + \tilde{D}^{PQ,RS}_{1,1}\rho\sigma_x\sigma_y \tag{18}$$

where

$$\tilde{D}^{PQ,RS}_{k,n-k} = \frac{1}{n!}\binom{n}{k} \frac{\partial^n \tilde{R}^{SPM}_{PQ,RS}}{\partial s_x{}^k \, \partial s_y{}^{n-k}}\bigg|_{s_x = s_y = 0} \quad , \tag{19}$$

and $\tilde{\chi}_{PQ}$ are evaluated in $\vartheta_i, \vartheta_s, \varphi_s$. Expressions of the derivatives in (19) will be illustrated in [12].

4. NUMERICAL RESULTS

We here present some numerical results relative to the bistatic NRCS in circular polarization basis, which are of interest for some recently proposed bistatic passive radar systems with GNSS signals of opportunity [14-15].

In Fig.2 we show the RL and RR NRCSs at L band, upwind, wind speed 10 m/s, at 45° incidence angle as functions of the scattering angle for different azimuth scattering angles. In Fig.3, dependence of these NRCSs on wind direction is illustrated. Our results can be compared with those of [16, Figs.8-9], obtained via the first and second order small slope approximation (SSA1 and SSA2). It can be verified that our results are in much better agreement with those of the more refined SSA2, although the latter requires fourfold numerical integrations, whereas our formulation is in closed form.

5. CONCLUSION

In this work, the monostatic A-PTSM introduced in [7] has been generalized to the bistatic case and applied to scattering from the sea surface, modelled by using the directional Elfouhaily spectrum and an anisotropic jointly Gaussian distribution of surface slopes. Closed-form

expressions of all the elements of the polarimetric covariance matrix, including NRCSs, have been obtained. The comparison of numerical results with those of other, more refined but less efficient, methods confirms the validity of the presented approach.

6. REFERENCES

[1] G. R. Valenzuela, "Scattering of Electromagnetic Waves from a Tilted Slightly Rough Surface", *Radio Sci.*, vol. 3, pp. 1057-1066, 1968.

[2] J. W. Wright, "A New Model for Sea Clutter", *IEEE Trans. Antennas Propag.*, vol. 16, pp. 217-223, 1968.

[3] F. T. Ulaby, R. K. Moore, and A. K. Fung, *Microwave Remote Sensing*. Reading, MA: Addison-Wesley, 1982.

[4] A. Iodice, A. Natale, and D. Riccio, "Retrieval of Soil Surface Parameters via a Polarimetric Two-Scale Model", *IEEE Trans. Geosc. Remote Sens.*, vol. 49, no. 7, pp. 2531-2547, July 2011.

[5] A. Iodice, A. Natale, and D. Riccio, "Polarimetric two-scale model for soil moisture retrieval via dual-pol HH-VV SAR data," *IEEE J. Sel. Topics Appl. Earth Observ.*, vol. 6, no. 3, pp. 1163–1171, Jun. 2013.

[6] G. Di Martino, A. Iodice, A. Natale, D. Riccio, "Polarimetric Two-Scale Two-Component Model for the Retrieval of Soil Moisture Under Moderate Vegetation via L-Band SAR Data", *IEEE Trans. Geosc. Remote Sens.*, vol.54, no.4, pp. 2470-2491, 2016.

[7] G. Di Martino, A. Iodice, D. Riccio, "Closed-Form Anisotropic Polarimetric Two-Scale Model for Fast Evaluation of Sea Surface Backscattering", *IEEE Trans. Geosc. Remote Sens.*, vol.57, no.8, pp. 6182-6194, 2019.

[8] G. Di Martino, A. Di Simone, A. Iodice, D. Riccio, "Closed-form Polarimetric Two-Scale Model for sea scattering evaluation," *2019 IEEE 5th International forum on Research and Technology for Society and Industry (RTSI)*, Florence, Italy, pp. 34-38, 2019.

[9] T. Elfouhaily, B. Chapron, K. Katsaros, and D. Vandemark, "A unified directional spectrum for long and short wind-driven waves," *J. Geophys. Res.*, vol. 102, pp. 15781–15796, 1997.

[10] C. S. Cox and W. Munk, "Measurement of the roughness of the sea surface from photographs of the sun's glitter", *J. Opt. Soc. Am.*, vol. 44, pp. 838–850, 1954.

[11] S. J. Katzberg, O. Torres, G. Ganoe, "Calibration of reflected GPS for tropical storm wind speed retrievals", *Geophys. Res. Lett.*, vol.33, L18602, pp. 1-5, 2006.

[12] G. Di Martino, A. Di Simone, A. Iodice, D. Riccio, "Bistatic scattering from anisotropic rough surfaces via the Polarimetric Two-Scale Model", *IEEE Trans. Geosc. Remote Sens.*, submitted.

[13] J.-S. Lee and E. Pottier, *Polarimetric Radar Imaging: From Basics to Applications*. Boca Raton, FL, USA: CRC Press, 2009.

[14] A. Di Simone et al. "Spaceborne GNSS-Reflectometry for Ship-Detection Applications: Impact of Acquisition Geometry and Polarization" *2018 IEEE International Geoscience and Remote Sensing Symposium* pp. 1071-1074, 2018.

[15] F. Santi, F. Pieralice, D. Pastina, "Joint detection and localization of vessels at sea with a GNSS-based multistatic radar," *IEEE Trans. Geosci. Remote Sens.*, vol. 57, no. 8, pp. 5894 - 5913, Aug. 2019.

[16] A. G. Voronovich and V. U. Zavorotny, "Full-polarization modeling of monostatic and bistatic radar scattering from a rough sea surface", *IEEE Trans. Antennas Propag.*, vol. 62, no. 3, pp. 1362–1371, March 2014.

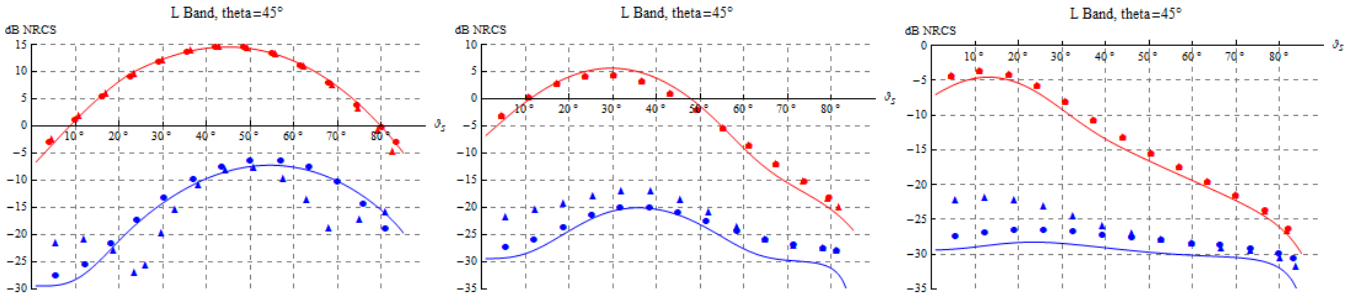

(a) (b) (c)

Figure 2: RL (red) and RR (blue) NRCS vs. the scattering angle ϑ_s at L band (frequency = 1.575 GHz, $\varepsilon = 75–j61$), $\vartheta_i = 45°$, and u_{10} = 10 m/s, upwind (φ_w=0), for $\varphi_s = 0$ (a), $\varphi_s = 30°$ (b), $\varphi_s = 60°$ (c). The results obtained with the SSA1 and SSA2 models are reported as triangles and dots (*RR* in blue and *RL* in red), respectively.

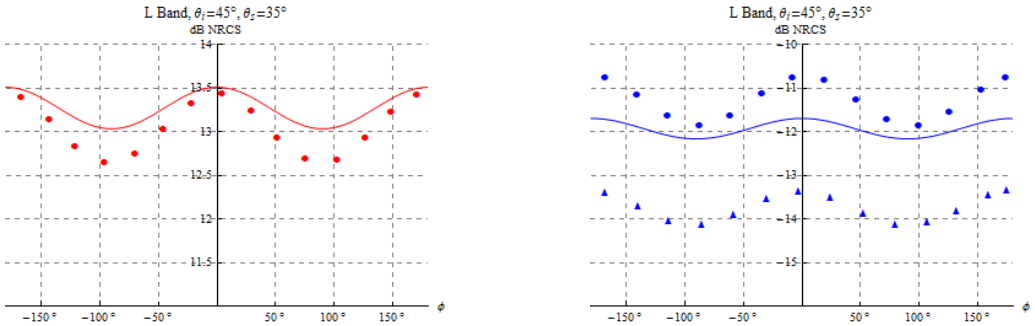

Figure 3: RL (left, red) and RR (right, blue) NRCS vs. wind direction φ_w at L band, for $\vartheta_i = 45°$, $\vartheta_s = 35°$, φ_s=0, u_{10} = 10 m/s. The results obtained with the SSA1 and SSA2 models are reported as triangles and dots (*RR* in blue and *RL* in red), respectively. SSA1 and SSA2 graphs are almost coincident for the RL NRCS.